Encapsulated fluorescent dyes

DOI: 10.1002/smll.200600319

Self-Assembly of Ultrabright Fluorescent Silica Particles**

Igor Sokolov, Yaroslav Y. Kievsky, and Jason M. Kaszpurenko*

Fluorescent particles have broad applications in tagging, tracing, and labeling.[1–5] Fluorescence is typically generated through incorporation of either inorganic or organic fluorescent dyes into the particle's material. While inorganic dyes are typically more stable, their number and compatibility is rather restricted. The large variety of organic dyes makes them attractive for creating fluorescent particles. However, the problems are in the stability and typically high toxicity of these dyes. Incorporation of dyes into a silica matrix seems to be one of most promising approaches because of the excellent sealing ability of silica and wide compatibility of silica with other materials. Numerous attempts to embed organic dyes into silica xerogels and zeolites have been made for a long time.[6–15] To prevent leakage of the dyes out of the porous matrix, the dyes were covalently bound to the silica matrix.[9,11,16–18] While the photostability of such materials was higher than the stability of pure dyes, it did not prevent bleaching substances, including oxygen, from penetrating inside such composite materials. In the case of xerogels, it is rather hard to use them for labeling. Recently there have been several reports about the incorporation of fluorescent lasing dyes into mesoporous patterned silica films[19] and silica roads.[20] Here we describe a novel synthesis of mesoporous silica particles with encapsulated organic dyes, in which the dyes are physically entrapped inside a silica matrix, through a one-step self-assembly process. We also demonstrate the encapsulation of a mixture of different dyes within single silica particles. The dyes are physically encapsulated inside nanosize channels/tubes in micrometer-size particles. Particles of such size can be of particular use in a number of applications, including flow cytometry and the labeling of skincare products.[21] Encapsulation is manifested through virtually no leakage of the dyes out of the particles. High concentrations of the fluorescent dyes can be reached inside the pores without dimerization of the fluorescent molecules. This results in fluorescence that is up to $\approx$500 times brighter than the maximum obtained from the same dye dissolved in aqueous solution at its maximum concentration before self-quenching (due to dimerization). By comparing this fluorescence with that observed for the brightest micrometer-size particles assembled from aqueous-compatible quantum dots[22] encapsulated in polymeric particles of similar size ($\approx$1.2 μm) reported recently,[23] one finds that the particles presented here (scaled to the same size) are about 170 times brighter. The fluorescence of the assembled particles is very stable.

To synthesize the mesoporous silica particles, the process of self-organization of mesoporous silica through acidic cationic surfactant templating and condensation of a silica precursor was used.[24,25] The dyes are added at the beginning of the synthesis at concentrations ($1–20\times10^{-3}$ M) that are substantially higher than the dimerization concentration of the fluorescent molecules ($\approx0.5\times10^{-4}$ M). It is interesting to note that the dyes are still dimerized in the synthesis solution, while we do not see any dimerization in the final product, the silica particles with encapsulated dyes (dimerization of the dyes can easily be detected by broadening of the fluorescence and, especially, absorbance peaks).

It is known[24,25] that the type of the synthesis used here results in a hexagonal array of pores/channels, which is typical for MCM-41 (or SBA-3 in another classification[26]) material. Small-angle X-ray scattering analysis (SAXS; not shown) shows that we are dealing with a mesoporous material with an interchannel distance of about 4 nm, which is the same as reported previously.[24,25] The most important feature of our synthesis is the morphology of the assembled material. This morphology consists of particles with specific shapes, mostly "discoids" and "gyroids" with a size on the order of a few micrometers (Figure 1a). Typical dimensions of the discoids/gyroids are 5–10 μm. One can also see some fiber shapes. The fibers, typically, are noticeably larger than the discoids/gyroids. Therefore, it is not difficult to separate them if necessary by either filtering or fluidic separation (Figure 1b,c). The inset in Figure 1a shows a zoomed image of a couple of particles that have a specific "ray" type of defect on their surfaces. Such defects have already been reported[24,25,27] and are the manifestation of closed channels/pores running along the circumference around the axis of symmetry of the particles. Certainly, this is indirect evidence of having closed pores. More direct proof can be obtained by analysis of the diffusion of the dyes out of the particles. It makes sense to compare diffusion out of our particles with diffusion out of particles that are known to have open channels/pores. The synthesis of well-characterized open-channel fibers with the same type of symmetry of channels and about the same microsize (2×5 μm) as our particles has been reported recently.[28] We used that synthesis but added the same amount of dye (rhodamine 6G, R6G) as was used for the synthesis reported here. As a result, we collected open-channel fibers with the dye inside the channels. The fibers were collected with a cone filter (0.5-μm open pore) and continuously washed for two minutes with distilled (DI) water. Our "closed-channel" particles, the discoids/gyroids, were collected and washed in exactly the same way. After that, the open-channel fibers were put in DI water in a cuv-

[*] Prof. I. Sokolov
Department of Physics, Department of Chemistry, and
Center for Advanced Material Processing (CAMP)
Clarkson University, Potsdam, NY 13699-5820 (USA)
Fax: (+1) 315-268-6610
E-mail: isokolov@clarkson.edu
Dr. Y. Y. Kievsky, J. M. Kaszpurenko
Department of Physics
Clarkson University, Potsdam, NY 13699-5820 (USA)

[**] This work was supported by the US Army Research Office (grant W911NF-05-1-0339).

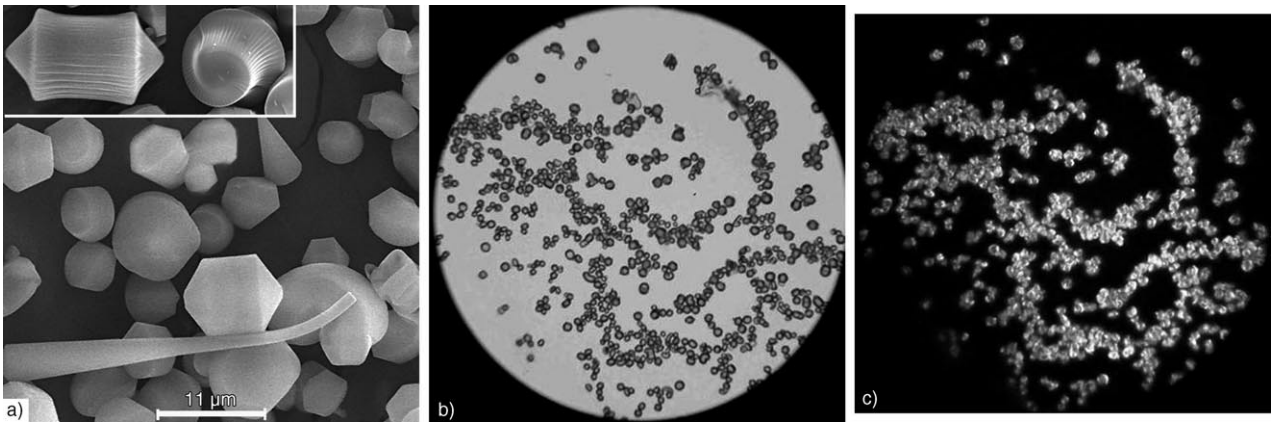

Figure 1. a) Scanning electron microscopy (SEM) image showing the variety of shapes of synthesized mesoporous particles. One can see discoids/gyroids and fiber shapes. The particles shown in the inset demonstrate the specific "ray" type of defect found on some particles. b, c) Optical images of the assembled discoids/gyroids: b) transmitted image and c) fluorescence image of the particles with encapsulated rhodamine 6G dye.

ette for UV/Vis spectroscopy. Approximately the same amount of our particles was placed in another cuvette with DI water. The amount of dye that has diffused out can be characterized by measuring the absorbance at a specific wavelength. Figure 2 shows the absorbance at a wavelength

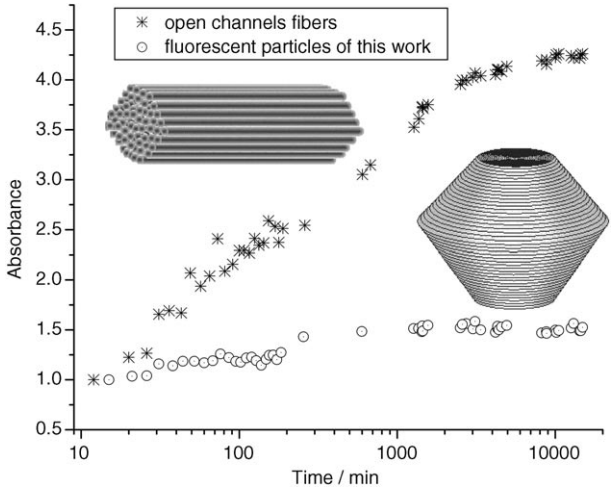

Figure 2. Absorbance (proportional to concentration) of the rhodamine 6G dye accumulated in water from diffusion out of open-channel fibers (stars) and from the fluorescent particles assembled here (circles). An open-pore fiber and a closed-pore discoid are shown schematically.

of 525 nm for both types of particle as a function of time. One can see that the dye diffuses much slowly from our particles than from the similarly sized channels in the open-channel fibers. Some initial leakage from the discoids/gyroids can probably be explained by surface scratching and cracks that developed in some particles during the filtering, washing, and resuspension in water. The possibility that there is some percentage of open channels/pores also cannot be excluded. On a longer timescale, we monitored both types of particle stored in clean DI water for a period of more than 18 months and observed virtually no change of color of our discoids/gyroids, while the open-channel fibers become colorless quite quickly.

For the sake of accuracy, it should be noted that the chemistry inside the pores of the two types of particle was not precisely the same. The acidity during synthesis was different and formamide was used in our synthesis. While formamide, being a solvent, is expected to facilitate diffusion and, consequently, increase the difference in the diffusion rates observed in Figure 2, the effect of the pH value can be more complicated. Nevertheless, in both syntheses we used a pH value below the isoelectric point of silica. Therefore, we expect that the nature of the electrostatic interactions between molecules of dye and the silica wall inside the pores does not change during the synthesis. In any case, the results shown in Figure 2 should be treated qualitatively.

To confirm that we are presumably dealing with dye physically encapsulated inside the nanochannels, another simple experiment was carried out. Particles, collected in the same way as for the diffusion experiment described above, were slightly crushed with a glass pipette. This should open more channels and let the dye diffuse out of the particles much faster. As expected, the visually observed amount of released dye was comparable with that released from open-channel fibers processed in the same way.

To find the concentration of the dye molecules inside the nanoporous silica, we used a 50% dimethylformamide (DMF) aqueous solution together with ultrasonic treatment to extract the dye molecules from the pores. It should be noted that such treatment results in partial destruction of the silica particles, which presumably opens all of the channels. The nature of this destruction is not completely clear, although we would expect this is due to penetration of DMF molecules through micropores/defects into the channels, which would create excessive osmotic pressure that can destroy the closed pores. The concentration of rhodamine 6G found inside the nanoporous silica particles was about 4×10^{-2} M. It is worthwhile mentioning a recent report of the encapsulation of dyes inside zeolites, where a similar

effect was observed and 10-times-higher concentrations of dye monomers were reported.[12] By using the pore geometry of these particles,[24,25] one can estimate that the above concentration corresponds to a distance of ≈3 nm between the dye molecules inside the pores. A sketch of such a configuration is presented in Figure 3.

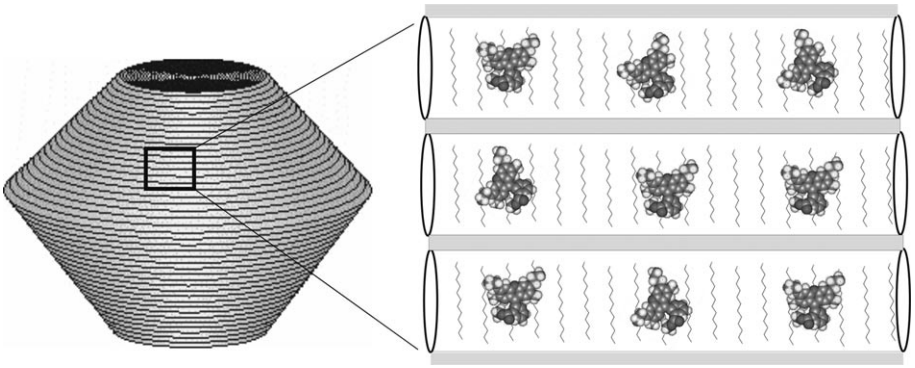

Figure 3. Schematic representation of the location of the dye molecules inside the synthesized shapes. The right side of the image presents an enlarged area with the dye encapsulated inside ≈3-nm channels. Alkane chains of surfactant molecules (shown as zigzag vertical lines with the head groups adjacent to silica walls) act as separators between the dye molecules and prevent dimerization of the dye molecules in the direction along the channels. In the perpendicular direction, the silica walls play the role of the separator to prevent dimerization.

To describe the fluorescence activity of the particles, we first used confocal microscopy and fluorometry. The confocal microscope (Nikon C1, 543 nm laser, 100× NA 1.4 objective) allows focusing of the laser light within a volume less then a cubic micrometer. By placing both particle and dye solutions at the maximum concentration (5×10^{-5} M) on a glass slide, one can compare the fluorescence signal coming out from inside the particle and from a similar volume of the dye solution. Such a direct comparison showed a ≈200-times-higher signal coming from the particles than from dye solution. This is in good agreement with the comparison made by using the fluorescence spectroscope (see below).

To compare the fluorescence brightness for the other excitation wavelengths and to find the quantum efficiency of the encapsulated dyes, we used fluorescence and UV/Vis spectrometers. The spectra for the solution of R6G dye and for R6G dye in the particles are shown in Figure 4. To compare the fluorescence coming from the same volume of the dye solution and the particle bulk, we first found the volume of the particles. To decrease the scattering effect of the particles, we used a fairly low concentration of the particles in suspension (9×10^{-3} vol.%; further decrease of the concentration below that leads to a linear change of the fluorescence signal). Fluorescence was recorded with all parameters of the spectrometer kept the same. To compare the signals from the dye and the particles, we multiplied the signal collected from the particles by the ratio of volumes of water and particle in the particle suspension. By comparing absolute maxima, one can see that the particles are ≈800-times more fluorescent than the aqueous solution of dye at a concentration of 3×10^{-5} M. This corresponds to ≈500-times the R6G dye maximum at its maximum nondimerized concentration of $\approx5\times10^{-5}$ M.

By comparing our particles with the encapsulated quantum dots reported recently,[23] one can make the following simple estimation. Each reported ≈1.2-μm polymeric particle contains $\approx5\times10^{4}$ quantum dots. Our particles of similar size contain $\approx1.7\times10^{8}$ molecules of R6G dye. According to Refs. [29,30], a single ZnS-capped CdSe quantum dot is ≈20 times brighter than a molecule of R6G. This brings the brightness of our particles to ≈170 times higher than the encapsulated quantum dots. The exact proportion depends on some other parameters, for example, on the refractive index of the particle itself (this determines how much light penetrates inside the particles).

By comparing the fluorescence and absorbance, one can estimate the quantum yield of dye inside the pores of the silica particles. By following Ref. [31] and using R6G at a concentration of 3×10^{-6} M as a reference, we estimated the quantum yield to be ≈10% (excitation wavelength of 488 nm). It is interesting to analyze this value: One finds that the ratio of the integral fluorescence of the particles (9×10^{-3} vol% concentration) to the dye solution (3×10^{-6} M concentration) is about 1/16 for 488-nm excitation. By using the found dye concentration in the synthesized particles (4×10^{-2} M) and taking the quantum yield of R6G to be equal to 95%, with the assumption of no dimerization and no change of quantum yield of the dye inside the particle pores, one could expect the quantum yield of the dye inside the particle to be ≈5% ($95\times1/16\times1/(9\times10^{-5})\times3\times10^{-6}/(4\times10^{-2})$), which is fairly close to the previous estimation. Both of these estimations, however, do not take into account the strong scattering of excitation light by silica particles, which is clearly seen in Figure 4b. The same scattering brings about a broad spectral decrease of transmitted light, which is seen as an elevated background signal in the absorbance plot for the particles (Figure 4c). If we subtract this background from the particle absorbance value, to leave presumably only the dye-specific absorbance, we get a quantum yield of ≈90% for the dye inside the particles. This implies that the quantum yield of the encapsulated dye is virtually unchanged as compared to that of the dye in water, that is, spectroscopically, the encapsulated dye is free inside the channels, and we are presumably dealing with just physical encapsulation (a more precise consideration of the scattered light will be studied in future work).

The increase in fluorescence comes from attaining higher concentrations of the dye molecules inside the pores without dye dimerization (which would quench fluores-

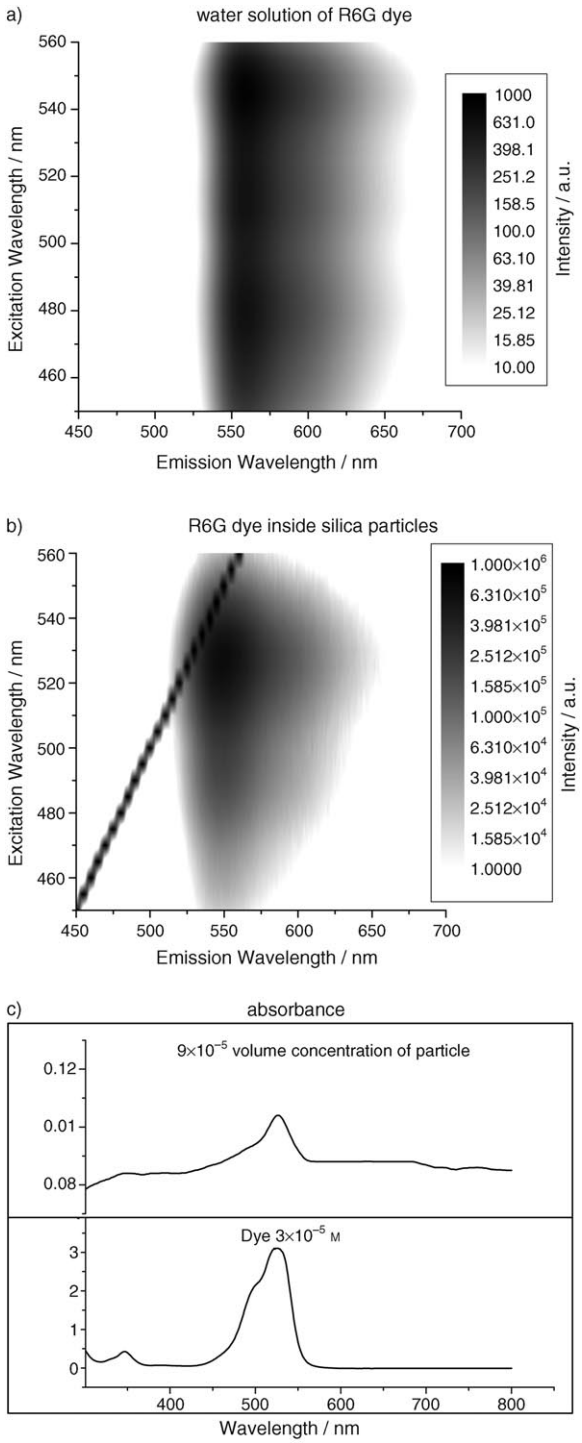

Figure 4. Fluorescence spectra of a) R6G dye in aqueous solution at a concentration of 3×10^{-5} M and b) R6G dye encapsulated in silica particles at a concentration of 9×10^{-3} vol%. The fluorescence signal is scaled up proportionally to 100% silica particles (as if it were just 100% volume silica particles). c) The absorbance spectra of both solutions.

cence). Maintenance of high concentrations of the dye without dimerization can presumably be explained by the presence of surfactant molecules inside the channels, which can act as dispersants (see Figure 3). Also, the silica walls between the channels naturally do not let the dye molecules dimerize in directions perpendicular to the channels. Potentially, interaction with the silica surface could also decrease fluorescence. Interaction of the dye molecules with the silica wall is diminished by the fact that the silica wall is coated with the surfactant head groups. While detailed analysis is shown here for the rhodamine 6G dye, similar results are observed for other rhodamine dyes; those will be published in detail in the future. By using a mix of several dyes in one synthesis, one gets a mixture of dyes, virtually a new color, inside each particle. Simple estimation shows that the number of such combinations of dyes is practically unlimited. The fluorescence of these particles is very stable. Finally, the particles are large enough (several micrometers) to be used as ultrabright fluorescent markers/labels in a broad variety of applications without the use of special fluorescence microscopes, since the particles are visible with rather basic instruments. The particles seem to be the brightest fluorescent particles synthesized so far.

Experimental Section

To synthesize mesoporous silica particles, we used the Origami type of synthesis[24,25] with the addition of fluorescent lasing dyes. The materials used were tetraethylorthosilicate (TEOS, *99.99+%*, Aldrich), cetyltrimethylammonium chloride (CTACl, 25 wt.% aqueous solution, Pflatz & Bauer), formamide (*99%*, Aldrich), hydrochloric acid (37.6 wt.% aqueous solution, SafeCote), and rhodamine 6G perchlorate dye (Sigma-Aldrich). All chemicals were used as received.

Synthesis: The surfactant, acid, dye, formamide, and distilled water (Corning, AG-1b, 1 MΩ cm) were stirred in a polypropylene bottle at room temperature for 2 h, after which TEOS was added and the solution stirred for approximately 5 min. The solution was then kept under quiescent conditions for 3 days. The molar ratio of H_2O:HCl:formamide:CTACl:TEOS:R6G was $100:7.8:9.5:0.11:0.13:6 \times 10^{-4}$–0.01. The materials so formed were filtered, washed with copious amounts of water, and air dried.

Keywords:

encapsulation · fluorescent dyes · self-assembly · silica

[1] U. Hasegawa, S. I. Nomura, S. C. Kaul, T. Hirano, K. Akiyoshi, *Biochem. Biophys. Res. Commun.* **2005**, *331*, 917–921.
[2] B. S. Edwards, T. Oprea, E. R. Prossnitz, L. A. Sklar, *Curr. Opin. Chem. Biol.* **2004**, *8*, 392–398.
[3] G. Lizard, S. Monier, C. Prunet, L. Duvillard, P. Gambert, *Ann. Biol. Clin.* **2004**, *62*, 47–52.
[4] M. Meldal, *Biopolymers* **2002**, *66*, 93–100.
[5] H. Ohata, H. Yamada, T. Niioka, M. Yamamoto, K. Momose, *J. Pharmacol. Sci.* **2003**, *93*, 242–247.
[6] A. P. Rao, A. V. Rao, *Mater. Lett.* **2003**, *57*, 3741–3747.
[7] A. M. Klonkowski, K. Kledzik, R. Ostaszewski, T. Widernik, *Colloids Surf. A* **2002**, *208*, 115–120.
[8] A. V. Deshpande, U. Kumar, *J. Non-Cryst. Solids* **2002**, *306*, 149–159.

[9] N. Leventis, I. A. Elder, D. R. Rolison, M. L. Anderson, C. I. Merzbacher, *Chem. Mater.* **1999**, *11*, 2837 – 2845.
[10] F. del Monte, D. Levy, *J. Phys. Chem. B* **1998**, *102*, 8036 – 8041.
[11] T. Suratwala, Z. Gardlund, K. Davidson, D. R. Uhlmann, J. Watson, N. Peyghambarian, *Chem. Mater.* **1998**, *10*, 190 – 198.
[12] G. Calzaferri, S. Huber, H. Maas, C. Minkowski, *Angew. Chem.* **2003**, *115*, 3860 – 3888; *Angew. Chem. Int. Ed.* **2003**, *42*, 3732 – 3758.
[13] H. Ow, D. Larson, M. Srivastava, W. W. Webb, B. Baird, U. Wiesner, *Abstr. Pap. Am. Chem. Soc.* **2003**, *225*, U639 – U639.
[14] X. J. Zhao, R. P. Bagwe, W. H. Tan, *Adv. Mater.* **2004**, *16*, 173 – 176.
[15] S. Santra, J. Xu, K. Wang, W. Tan, *J. Nanosci. Nanotechnol.* **2004**, *4*, 590 – 599.
[16] R. Frantz, C. Carbonneau, M. Granier, J. O. Durand, G. F. Lanneau, R. J. P. Corriu, *Tetrahedron Lett.* **2002**, *43*, 6569 – 6572.
[17] G. A. Baker, S. Pandey, E. P. Maziarz, F. V. Bright, *J. Sol-Gel Sci. Technol.* **1999**, *15*, 37 – 48.
[18] Y. S. Lin, C. P. Tsai, H. Y. Huang, C. T. Kuo, Y. Hung, D. M. Huang, Y. C. Chen, C. Y. Mou, *Chem. Mater.* **2005**, *17*, 4570 – 4573.
[19] P. Yang, G. Wirnsberger, H. C. Huang, S. R. Cordero, M. D. McGehee, B. Scott, T. Deng, G. M. Whitesides, B. F. Chmelka, S. K. Buratto, G. D. Stucky, *Science* **2000**, *287*, 465 – 467.
[20] F. Marlow, M. D. McGehee, D. Zhao, B. F. Chmelka, G. D. Stucky, *Adv. Mater.* **1999**, *11*, 632 – 636.
[21] S. Iyer, Y. Kievsky, I. Sokolov, *Skin Res. Technol.* **2006**, *12*, 1 – 6.
[22] H. Ow, D. R. Larson, M. Srivastava, B. A. Baird, W. W. Webb, U. Wiesner, *Nano Lett.* **2005**, *5*, 113 – 117.
[23] M. Y. Han, X. H. Gao, J. Z. Su, S. Nie, *Nat. Biotechnol.* **2001**, *19*, 631 – 635.
[24] I. Sokolov, Y. Kievsky, *Stud. Surf. Sci. Catal.* **2005**, *156*, 433 – 443.
[25] S. M. Yang, I. Sokolov, N. Coombs, C. T. Kresge, G. A. Ozin, *Adv. Mater.* **1999**, *11*, 1427 – 1431.
[26] T. R. Pauly, Y. Liu, T. J. Pinnavaia, S. J. L. Billinge, T. P. Rieker, *J. Am. Chem. Soc.* **1999**, *121*, 8835 – 8842.
[27] N. Coombs, D. Khushalani, S. Oliver, G. A. Ozin, G. C. Shen, I. Sokolov, H. Yang, *J. Chem. Soc. Dalton Trans.* **1997**, 3941 – 3952.
[28] Y. Kievsky, I. Sokolov, *IEEE Trans. Nanotechnol.* **2005**, *4*, 490 – 494.
[29] W. C. W. Chan, S. M. Nie, *Science* **1998**, *281*, 2016 – 2018.
[30] W. C. W. Chan, D. J. Maxwell, X. H. Gao, R. E. Bailey, M. Y. Han, S. M. Nie, *Curr. Opin. Biotechnol.* **2002**, *13*, 40 – 46.
[31] A. T. R. Williams, S. A. Winfield, J. N. Miller, *Analyst* **1983**, *108*, 1067 – 1071.

Received: June 29, 2006
Revised: September 18, 2006
Published online on January 24, 2007

